

Controlling discrete quantum walks: coins and initial states

Ben Tregenna,¹ Will Flanagan,¹ Rik Maile,¹ and Viv Kendon^{1,2,*}

¹*Optics Section, Blackett Laboratory, Imperial College, London, SW7 2BW, United Kingdom.*

²*Mathematical Sciences Research Institute, 1000 Centennial Drive, Berkeley, CA 94720-5070, USA*

(Dated: May 13, 2003)

In discrete time, coined quantum walks, the coin degrees of freedom offer the potential for a wider range of controls over the evolution of the walk than are available in the continuous time quantum walk. This paper explores some of the possibilities on regular graphs, and also reports periodic behaviour on small cyclic graphs.

I. INTRODUCTION

Quantum walks are analogs of classical random walks, designed primarily with the aim of finding quantum algorithms that are faster than classical algorithms for the same problem. There are two distinct types of quantum walks, corresponding to classical random walks with discrete or continuous time (but both taking place in a discrete space). Continuous time quantum walks were first introduced in 1997 by Farhi and Gutmann [1]. Discrete time quantum walks with a quantum coin appeared in the early 1990s in work by Y Aharonov *et al.* [2], then were developed as quantum cellular automata by Meyer [3, 4, 5] in 1996. The first explicitly algorithmic context for coined quantum walks came from D Aharonov *et al.* [6] and Ambainis *et al.* [7] in 2000.

Two algorithms for quantum walks have recently been presented. Childs *et al.* [8] prove that a continuous time quantum walk can find its way across a special type of graph exponentially faster than any classical algorithm, and Shenvi *et al.* [9] prove that a discrete time, coined quantum walk can equal Grover's search algorithm, by finding a marked item in an unsorted database with a quadratic speed up over the best known classical algorithm. These results are extremely promising, but still a long way from the diversity of problems that classical random walks provide the best known solutions for, such as approximating the permanent of a matrix [10], finding satisfying assignments to Boolean expressions (k SAT with $k > 2$) [11], estimating the volume of a convex body [12], and graph connectivity [13]. Classical random walks underpin many standard methods in computational physics, such as Monte Carlo simulations, so a more efficient quantum alternative would presumably widen the potential application of quantum computers to problems in physics.

In much the same way as we now know almost everything about the properties and possible states of two qubits, though quantum computers will clearly need far more than two qubits to be useful, the simple quantum walk on a line has now been well studied, see for example Refs. [7, 14, 15, 16, 17, 18, 19], though there is no sugges-

tion that it will lead to useful quantum walk algorithms by itself. The quantum walk on a cycle is a step closer to algorithms. The N -cycle is the Cayley graph of the cyclic group of size N , and in addition to proving that the coined quantum walk on a cycle has a time-averaged mixing time almost quadratically faster than a classical random walk, D Aharonov *et al.* [6] also provided a lower bound on the time-averaged mixing times for quantum walks on general graphs of bounded degree, suggesting a quadratic improvement over classical random walks is the best that can be achieved. Moore and Russell [20] solved both discrete and continuous time quantum walks on the hypercube of size N , showing that both have an instantaneous mixing time linear in N , logarithmically faster than classical random walks. However, they also showed that time-averaged mixing times on the hypercube are slower than classical, the continuous time walk never mixes in the sense of the time-averaged definition. Kempe [21] proved that a quantum walk can travel from one corner of a hypercube to the opposite corner exponentially faster than a classical random walk, however, there are other classical algorithms that can do this task efficiently so this does not provide a quantum advantage over classical. For a recent survey of quantum walks and a more complete list of references, see Kempe [22].

So far, though the published literature on discrete and continuous time quantum walks tends to treat different problems, the evidence suggests that both can accomplish the same tasks. They are clearly not exactly equivalent, and the computational equivalence observed depends on choosing an appropriate form for the coin operator for the discrete time walks. This raises the possibility that different choices of coin operator could perform other useful tasks that aren't easily accessible within the continuous time quantum walk model. In this paper, we present a study of the properties of different coin operators using both analytical and numerical methods. Our results are of interest both in themselves as examples of quantum dynamics, and as potential ingredients for quantum algorithms. The paper is organized as follows. After setting up our notation, we discuss the possibilities for graphs of degree two, three, and four in Secs. II, III, and IV respectively. In Sec. V we briefly mention graphs of higher degree and in Sec. VI we describe periodic quantum walks on cyclic graphs.

*Electronic address: Viv.Kendon@ic.ac.uk

A. Notation for a general quantum walk

A general coined quantum walk on a d -regular graph needs a coin Hilbert space, \mathcal{H}_d with d the degree of each vertex in the graph on which the walk takes place, and a position Hilbert space \mathcal{H}_N with N the number of vertices in the graph (which can be infinite). The dynamics of the walk are controlled by a coin flip operator \mathbf{C} that acts on the coin Hilbert space, and a conditional shift operator \mathbf{S} that shifts the particle position according to the state of the coin. Together, $\mathbf{U} \equiv \mathbf{S}(\mathbf{C} \otimes \mathbf{I}_N)$ is the unitary operator for one step of the walk. If the particle and coin start in state $|\psi_0\rangle$, the state of the system after t steps of the walk is $|\psi_t\rangle = \mathbf{U}^t |\psi_0\rangle$.

A powerful technique for the solution of classical random walks that generalises well to the quantum case is that of Fourier transformation. When the walk occurs on the Cayley graph of some group, the quantum walk simplifies greatly on consideration of the Fourier space of the particle [6, 7]. Quantum walks on the infinite line, N -cycle and the hypercube admit this type of solution. An alternative method using path counting (path integrals) was also presented in [7] and further refined in [15].

II. GRAPHS OF DEGREE TWO

We will consider the simplest examples first, coined quantum walks on the line and the cycle. The walk on the line has already been analysed in detail and the equivalence of all unbiased coin operators noted by several authors [7, 14, 16]. We first review these calculations, since the notation and results will be used in our analysis of the walk on the N -cycle.

A. Quantum walk on an infinite line

The most general two dimensional unitary coin operator $\mathbf{C}_2^{(\text{gen})}$ can be written as a 2×2 matrix

$$\mathbf{C}_2^{(\text{gen})} = \begin{pmatrix} \sqrt{\rho} & \sqrt{1-\rho}e^{i\theta} \\ \sqrt{1-\rho}e^{i\phi} & -\sqrt{\rho}e^{i(\theta+\phi)} \end{pmatrix}, \quad (1)$$

where $0 \leq \theta, \phi \leq \pi$ are arbitrary angles, $0 \leq \rho \leq 1$, and we have removed an irrelevant global phase so as to leave the leading diagonal element real. The Hadamard coin operator is obtained with $\rho = 1/2$ and $\theta = \phi = 0$. The parameter ρ thus controls the bias of the coin, $\rho = 1/2$ being a fair coin that chooses each of the two possible directions $|R\rangle$ (right) and $|L\rangle$ (left) with equal probability. Trivial cases $\rho = 0, 1$ give oscillatory motion and uniform motion respectively. The Fourier transformation is performed only over the particle Hilbert space,

$$|\tilde{\psi}(k, t)\rangle = \sum_x |\psi(x, t)\rangle e^{ikx}. \quad (2)$$

Here the state vectors $|\psi(x, t)\rangle$ and $|\tilde{\psi}(k, t)\rangle$ are two component vectors, with the first component being the amplitude of the right moving part and the second component being that of the left moving part, with $k \in [0, 2\pi)$. Using the general form of the coin transition matrix for a one dimensional walk, Eq. (1), a single step of the walk becomes

$$|\tilde{\psi}(k, t+1)\rangle = \mathbf{C}_k^{(\text{gen})} |\tilde{\psi}(k, t)\rangle, \quad (3)$$

where $\mathbf{C}_k^{(\text{gen})}$ is a 2×2 matrix acting on the coin Hilbert space,

$$\mathbf{C}_k^{(\text{gen})} = \begin{pmatrix} \sqrt{\rho}e^{ik} & \sqrt{1-\rho}e^{i(k+\theta)} \\ \sqrt{1-\rho}e^{i(-k+\phi)} & -\sqrt{\rho}e^{i(-k+\theta+\phi)} \end{pmatrix}. \quad (4)$$

This matrix may be diagonalised, yielding eigenvalues

$$\lambda_k^\pm = \pm e^{i\delta} e^{\pm i\omega_k}, \quad (5)$$

where $\delta = (\theta + \phi)/2$ and

$$\sin(\omega_k) = \sqrt{\rho} \sin(k - \delta). \quad (6)$$

The associated eigenvectors are

$$|\tilde{\xi}_k^\pm\rangle = \frac{1}{n_k^\pm} \begin{pmatrix} e^{ik} \\ e^{-i\theta}(\lambda_k^\pm - \sqrt{\rho}e^{ik})/\sqrt{1-\rho} \end{pmatrix}, \quad (7)$$

with the normalisation factor n_k^\pm given by

$$(n_k^\pm)^2 = 2 \{1 \mp \sqrt{\rho} \cos(k - \delta \mp \omega_k)\} / (1 - \rho) \quad (8)$$

For a general unbiased initial coin state, $|\psi(x, 0)\rangle = \sqrt{\eta}(|R\rangle + e^{i\alpha}\sqrt{1-\eta}|L\rangle) \otimes |0\rangle$, the Fourier components at $t = 0$ can be found from Eq. (2),

$$|\tilde{\psi}(k, 0)\rangle = \begin{pmatrix} \sqrt{\eta} \\ e^{i\alpha}\sqrt{1-\eta} \end{pmatrix} \otimes |k\rangle \quad \forall k. \quad (9)$$

Collecting all these pieces together, it is possible to write down the Fourier components at all later times t ,

$$|\tilde{\psi}(k, t)\rangle = (\mathbf{C}_k^{(\text{gen})})^t |\tilde{\psi}(k, 0)\rangle. \quad (10)$$

Expressing $\mathbf{C}_k^{(\text{gen})}$ in terms of its eigenvalues and eigenvectors, $(\mathbf{C}_k^{(\text{gen})})^t = (\lambda_k^+)^t |\tilde{\xi}_k^+\rangle \langle \tilde{\xi}_k^+| + (\lambda_k^-)^t |\tilde{\xi}_k^-\rangle \langle \tilde{\xi}_k^-|$, gives

$$|\tilde{\psi}(k, t)\rangle = (\lambda_k^+)^t |\tilde{\xi}_k^+\rangle \langle \tilde{\xi}_k^+ | \tilde{\psi}(k, 0)\rangle + (\lambda_k^-)^t |\tilde{\xi}_k^-\rangle \langle \tilde{\xi}_k^- | \tilde{\psi}(k, 0)\rangle \quad (11)$$

The coefficients of $|\tilde{\xi}_k^\pm\rangle$ are given by

$$(\lambda_k^\pm)^t \langle \tilde{\xi}_k^\pm | \tilde{\psi}(k, 0)\rangle = \frac{(\lambda_k^\pm)^t}{n_k^\pm} e^{-ik} \left\{ \sqrt{\eta} - \sqrt{\frac{1-\eta}{1-\rho}} e^{i(\theta+\alpha)} (\sqrt{\rho} \mp e^{i(k-\delta)} e^{\mp i\omega_k}) \right\}. \quad (12)$$

All the subsequent statistics for the probability distribution may be found by inverting the Fourier transform and

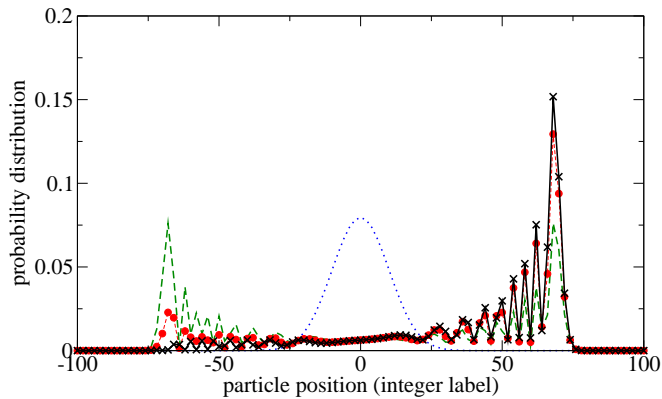


FIG. 1: Asymmetric distributions obtained with various initial states and Hadamard coin for the walk on a line after 100 steps: coin bias $\eta \simeq 0.85$ (crosses), coin state $|R\rangle$ (circles), with symmetric (dashed) and classical (dotted) for comparison. Only even-numbered positions are plotted, since the distribution is zero on odd-numbered positions.

applying standard methods from complex analysis [7, 15]. However, the question of the effect of the extra degrees of freedom α and η pertaining to the quantum coin, and ϕ , θ and ρ in the coin operator, may be answered directly from Eq. (12). The parameters η and ρ appear in a non-trivial way and thus affect the subsequent evolution of the walk, but the phase factor α occurs solely with the phase θ in the coin flip operator as the combination $(\theta + \alpha)$. The other influences on the evolution from the phases in the coin flip matrix come from the factor $e^{i\delta t}$ in the eigenvalues, which is a global phase and therefore doesn't affect observable quantities, and from phases of $e^{i(k-\delta)}$ (explicitly and in ω_k), which disappear when k is integrated over its full range during the inverse Fourier transform. Thus, for any given θ in the coin operator, one may choose an α so as to give the full range of possible evolutions. This has been noted by several authors, [7, 14, 16]. For the walk on a line, without loss of generality, one may thus restrict the coin operator to one with real coefficients, and obtain the full range of behaviour by choosing different initial coin states. Further restricting to unbiased coins ($\rho = 1/2$), the Hadamard coin

$$\mathbf{C}_2^{(H)} = \begin{pmatrix} 1 & 1 \\ 1 & -1 \end{pmatrix}, \quad (13)$$

is thus the only possible type of coin for the quantum walk on a line.

The asymmetry of the distribution obtained for an initial coin state of $|R\rangle$ or $|L\rangle$ is now well-known, and is also obtained for unbiased initial states with $\alpha = 0$ or π . However, it is possible to create an even more biased distribution using the Hadamard (unbiased) coin operator, by choosing a biased initial state with $\eta \simeq 0.85$, i.e., $|\psi_0\rangle = (\sqrt{0.85}|R\rangle + \sqrt{0.15}|L\rangle) \otimes |0\rangle$. This is shown in Fig. 1, along with the distributions for $|R\rangle$, and symmetric quantum and classical distributions for compar-

ison. The asymmetry of the distribution can be quantified by examining the third moment, which we take about the origin, i.e., with reference to the initial location of the particle, normalised by the second moment, $\langle x^3 \rangle / \langle x^2 \rangle^{3/2}$. This quantity is just greater than one for the initial state with $\eta \simeq 0.85$, and around 0.7 for an initial state of $|R\rangle$ (obtained numerically, for analytic formulae see Konno [23, 24], the value of η comes from $\cos(\pi/8) \simeq 0.85$). By simply changing the phase by π to $\sqrt{0.85}|R\rangle - \sqrt{0.15}|L\rangle$, the distribution becomes symmetric. Comparing this with the unbiased coin initial state $(|R\rangle + i|L\rangle)/\sqrt{2}$ that also gives a symmetric evolution, and noting that the Hadamard operator is real, so any component with phase i remains orthogonal to any real component, we can see that there are two distinct ways of arriving at a symmetric quantum walk on a line. Initial states $\sqrt{0.85}|R\rangle - \sqrt{0.15}|L\rangle$ (biased) and $(|R\rangle + i|L\rangle)/\sqrt{2}$ (symmetric) give almost identical probability distributions, but the former is obtained by interference and the latter by combining probabilities from two mirror image orthogonal components.

This gives us our first insights into how to use the coin to control the walk. The quadratic speed up in the spreading of the quantum walk over classical is unaffected by the choice of initial state or coin operator: the speed up comes solely from the coherent wave motion along the line. This is made clearest by noting that a maximally mixed initial coin state also produces a symmetric distribution like the previous two examples. We can then control whether (and to what degree) the waves will interfere constructively, destructively, or not at all, by choosing the phase and bias of the coin initial state.

B. Quantum Walk on a N -Cycle

The walk on a N -cycle is the same as the walk on the line but with the particle position taken as $x \pmod{N}$. It is also amenable to solution in the Fourier basis. The finite state space of the particle gives rise to a discrete, finite momentum space defined by

$$|\tilde{\psi}_N(k, t)\rangle = \frac{1}{\sqrt{N}} \sum_{x=0}^{N-1} |\psi_N(x, t)\rangle e^{2\pi i k x / N}, \quad (14)$$

for $k \in \{0, 1, \dots, N-1\}$. From here it is possible to proceed in a similar manner to that shown in Sec. II A for a walk on an infinite line. Equation (3) may be used again, with the discrete version of $\mathbf{C}_k^{(\text{gen})}$ given by

$$\mathbf{C}_k^{(N)} = \begin{pmatrix} \sqrt{\rho} e^{2\pi i k / N} & \sqrt{1-\rho} e^{i(2\pi k / N + \theta)} \\ \sqrt{1-\rho} e^{i(-2\pi k / N + \phi)} & -\sqrt{\rho} e^{i(-2\pi k / N + \theta + \phi)} \end{pmatrix}. \quad (15)$$

This may again be diagonalised, yielding eigenvalues

$$\lambda_k^\pm = \pm e^{i\delta} e^{\pm i\omega_k^{(N)}}, \quad (16)$$

where now

$$\sin(\omega_k^{(N)}) = \sqrt{\rho} \sin(2\pi k / N - \delta), \quad (17)$$

compare Eq. (6). The possible solutions for $\omega_k^{(N)}$ are bounded by $\sin^{-1}(\sqrt{\rho})$, e.g., for $\rho = 1/2$, there are two solutions for $\omega_k^{(N)}$ one in each of the regions $[\pi/4, 3\pi/4]$ and $[-\pi/4, -3\pi/4]$. The first solution corresponds to λ_k^+ and the second to λ_k^- .

Classically, a random walk on a cycle tends to a uniform distribution over all points on the cycle at long times. Since the quantum walk is unitary and reversible, it never reaches a uniform distribution, the initial state influences the particle's dynamics at all later times. However, we can define a time-averaged distribution [6] which does tend to a limiting value for large T ,

$$\bar{P}(x, T) = \frac{1}{T} \sum_{t=0}^{T-1} P(x, t), \quad (18)$$

where $P(x, t) = |U^t|\psi_N(x, 0)\rangle|^2$. It is proven in [6] that

$$\begin{aligned} \lim_{T \rightarrow \infty} \bar{P}(x, T) &= \sum_{v, u \in \lambda_v = \lambda_u} \langle \psi_N(x, 0) | \phi_v^\pm \rangle \langle \phi_u^\pm | \psi_N(x, 0) \rangle \\ &\times \sum_a \langle x, a | \phi_v^\pm \rangle \langle \phi_u^\pm | x, a \rangle, \end{aligned} \quad (19)$$

where the sum is taken only over degenerate eigenvectors of the position space evolution matrix \mathbf{U} , which are denoted by $|\phi_v^\pm\rangle$, $|\phi_u^\pm\rangle$, with eigenvalues $\lambda_v^\pm = \lambda_u^\pm$. The general initial state is once again $|\psi_N(x, 0)\rangle = \sqrt{\eta}(|R\rangle + e^{i\alpha}\sqrt{1-\eta}|L\rangle) \otimes |0\rangle$. For the walk on a N -cycle, the eigenvectors of \mathbf{U} in the position basis are given by $|\phi_v^\pm\rangle = |\xi_k^\pm\rangle \otimes |\chi_k\rangle$, where the $|\xi_k^\pm\rangle$ are the eigenvectors of the matrix $\mathbf{C}_k^{(N)}$ and $|\chi_k\rangle = \frac{1}{\sqrt{N}} \sum_x e^{2\pi i k x / N} |x\rangle$, i.e., a discrete Fourier transform of the usual particle position basis states. (We omit labels of N from $|\xi_k^\pm\rangle$ and $|\chi_k\rangle$ to keep the notation less cluttered.) The associated eigenvalues of \mathbf{U} are (by construction) equal to those of the matrices $\mathbf{C}_k^{(N)}$, namely λ_k^\pm . Hence we can rewrite Eq. (19) in terms of the eigenvectors of $\mathbf{C}_k^{(N)}$,

$$\begin{aligned} \lim_{T \rightarrow \infty} \bar{P}(x, T) &= \sum_{a, k, j, b, c} \langle \psi_N(x, 0) | \chi_k, \xi_k^b \rangle \langle \chi_j, \xi_j^c | \psi_N(x, 0) \rangle \\ &\times \langle x, a | \chi_k, \xi_k^b \rangle \langle \chi_j, \xi_j^c | x, a \rangle. \end{aligned} \quad (20)$$

The sum is taken over k, j, b and c such that $\lambda_k^b = \lambda_j^c$. It was shown in [6] that since the $|\chi_k\rangle$ induce a uniform distribution over the nodes, the limiting distribution will also be uniform if all eigenvalues are distinct. The eigenvalues are degenerate in the general case if there exist non-trivial solutions for

$$\sin(2\pi k/N - \delta) = \sin(2\pi j/N - \delta). \quad (21)$$

This equation has solutions $k = j$ and $k + j \pmod{N} = N/\pi(\delta + \pi/2)$. The first is trivial, but whether the second solution has roots depends on the coin flip operator and on N . For example, when a Hadamard coin is used, $\theta = \phi = \delta = 0$ so the condition becomes

$k + j \pmod{N} = N/2$ which has roots only for even N . Thus for a Hadamard walk, cycles with an odd number of nodes converge to the uniform distribution and those with an even number converge to a non-uniform distribution derived below. However, for a given N , the coin flip operator with $(\delta + \pi/2) = \pi/N$ gives roots when $k + j \pmod{N} = 1$ which always has a solution, leading to a non-uniform limiting distribution. Conversely, if δ is not a rational multiple of π , there can be no solutions, and so the walk will always mix to the uniform distribution. Thus, by appropriate choice of coin operator, a walk on any size cycle can be made to converge either to a uniform or to a non-uniform probability distribution. This is in direct contrast to the classical case, in which the properties of the limiting distribution depend solely on the form of the graph.

We note that the limit as the cycle size $N \rightarrow \infty$ leads to the condition $\delta = -\pi/2$ for a non-uniform limiting distribution. This gives $\theta + \phi = -\pi$, the simplest unbiased coin operator corresponding to this is

$$\mathbf{C}_2^{(\text{nu})} = \frac{1}{\sqrt{2}} \begin{pmatrix} 1 & -i \\ -i & 1 \end{pmatrix}. \quad (22)$$

However, the practical limit of infinite cycle size is the walk on a line, where the the opposite edges of the walk never meet, and conditions for non-uniform distributions are not meaningful.

It is possible to derive the limiting distribution when there exist degenerate eigenvalues of the evolution operator \mathbf{U} . In these cases, the summation in Eq. (20) contains two distinct types of terms, those for which $k = j$ and those for which $j = N/\pi(\delta + \pi/2) - k \equiv \Phi - k$,

$$\begin{aligned} \lim_{T \rightarrow \infty} \bar{P}(x, T) &= \sum_{a, k, b} \left[|\langle \psi_N(x, 0) | \chi_k, \xi_k^b \rangle|^2 |\langle x, a | \chi_k, \xi_k^b \rangle|^2 \right. \\ &+ \langle \psi_N(x, 0) | \chi_k, \xi_k^b \rangle \langle \chi_{\Phi-k}, \xi_{\Phi-k}^{-b} | \psi_N(x, 0) \rangle \\ &\times \langle x, a | \chi_k, \xi_k^b \rangle \langle \chi_{\Phi-k}, \xi_{\Phi-k}^{-b} | x, a \rangle \left. \right]. \end{aligned} \quad (23)$$

Using $|\langle x | \chi_k \rangle|^2 = 1/N$, $\sum_a |\langle a | \xi_k^b \rangle|^2 = 1$ and $\sum_{k, b} |\langle \psi_N(x, 0) | \chi_k, \xi_k^b \rangle|^2 = 1$, the first term is easily seen to be the uniform distribution ($1/N$). In the second term, the factor that determines the form of the limiting distribution is

$$\langle x | \chi_k \rangle \langle \chi_{\Phi-k} | x \rangle = e^{4\pi i x / N(k - N\delta/2\pi - N/4)}, \quad (24)$$

which controls the sign of the terms in the sums. When $x = 0$, all the terms in the summation are positive, leading to a spike in the distribution about the origin. Similarly, if $x = N/2$, the phase of each term is $2\pi(k - N\delta/2\pi - N/4)$ so the terms add coherently (remember $(N\delta/\pi - N/2)$ is an integer). Specifically, for the Hadamard coin, $\delta = 0$ and the contribution to the sum is positive if $N/2$ is even, i.e., N is divisible by four, or negative if $N/2$ is odd, leading to a minimum. The Hadamard case has been independently calculated in more detail by Bednarska *et al.* [25], who also explore some possibilities

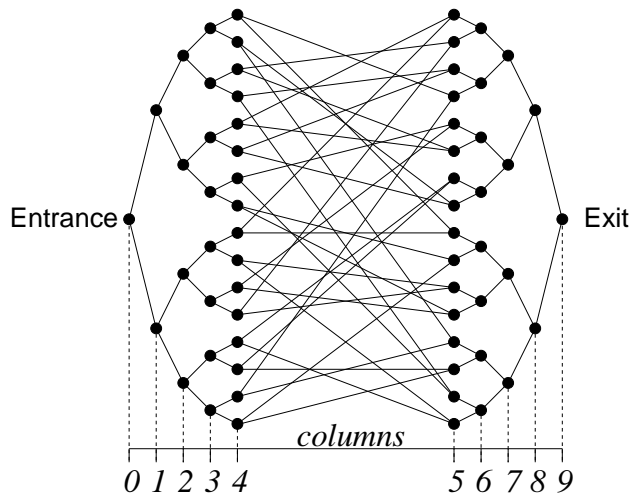


FIG. 2: “Glued trees” graph used in the algorithm of Ref. [8]. Example shown is for $N = 4$, with $2N + 1 = 9$ columns labeled at the bottom of the figure, and $2(2^{(N+1)} - 1) = 62$ nodes. The task is to travel from entrance to exit without getting lost in the randomly joined middle section of the graph. The gap between columns 4 and 5 is for clarity in the figure and is not significant in the algorithm.

for highly non-uniform limiting distributions generated by initial states superposing several particle positions.

The effects of different coin flip operators have received little attention in the literature to date, perhaps due to the minimal effect they have for a walk on a line. However, for quantum walks containing closed cycles, the choice of coin flip operator determines which phase the wavefronts have when they meet up with each other, selecting between whether constructive or destructive interference occurs. Note that in [17] it was shown that decoherence in a walk on a cycle causes all initial states and coin operators to mix to the uniform distribution even while there is still a clear quantum speed up over the classical mixing times. The coherence required for non-uniform limiting distributions is thus much more stringent than that required for a quantum speed up of the mixing time over classical. This suggests that in order to use the effects non-uniform limiting distributions it will be more useful if they have properties that can be measured after relatively few steps of the walk, rather than waiting for long times.

III. GRAPHS OF DEGREE THREE

Regular lattices of degree three have been studied briefly numerically [26], where the spreading rate was shown to be faster than classical. The “glued trees” graph used for the algorithm presented in Ref. [8] is also of degree three apart from the special start and end points that form the roots of the two binary trees, see Fig. 2. This structure is highly symmetric, despite the random connections in the middle, and provided a sym-

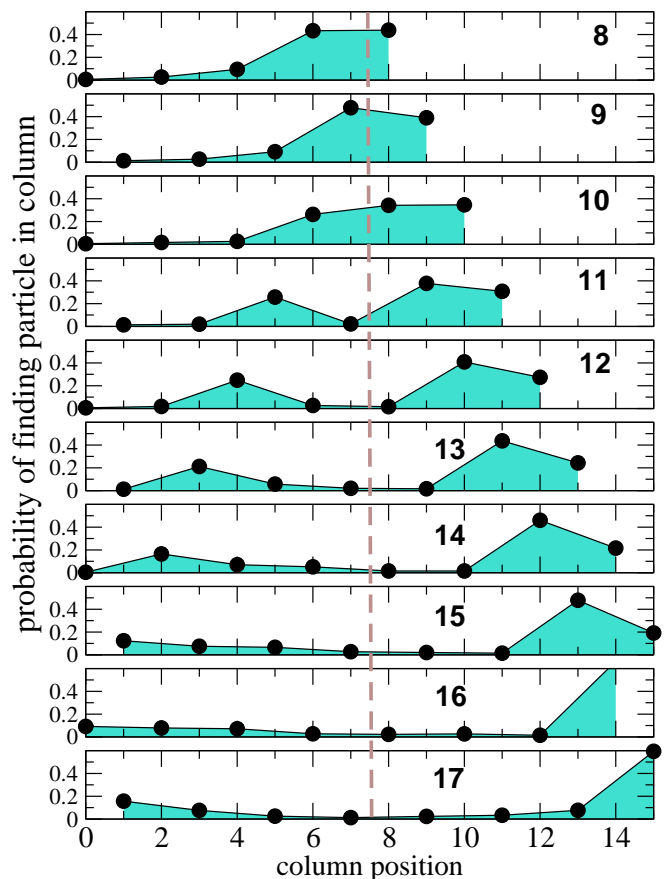


FIG. 3: Distribution over columns of the “glued trees” graph of Ref. [8] with a discrete time walk using a Grover coin. This is for a graph of size $N = 7$ (with $2N + 1 = 15$ columns). The vertical dashed line indicates the position of the random join between the two trees. The quantum walk reaches the far end in just 17 steps, with probability around 0.6 (same as the continuous time version).

metric initial state is used at the entrance node, the whole quantum walk process can be mapped to a walk on a line (the column positions shown in Fig. 2) with different biases in the probabilities for moving right or left at each step. Childs *et al.* [8] use a continuous time walk for their algorithm, but if a three dimensional coin based on Grover’s diffusion operator with elements $2/d - \delta_{ij}$,

$$\mathbf{C}_3^{(G)} = \frac{1}{3} \begin{pmatrix} -1 & 2 & 2 \\ 2 & -1 & 2 \\ 2 & 2 & -1 \end{pmatrix}, \quad (25)$$

is used with a discrete walk, the amplitude also interferes constructively in the right way to reach the opposite root of the trees quickly with high probability [17, 27], see Fig. 3.

The Grover coin is biased but symmetric. The DFT (discrete Fourier transform) coin is unbiased, but asymmetric in that you cannot interchange the labels on the directions without changing the coin operator. For $d = 3$,

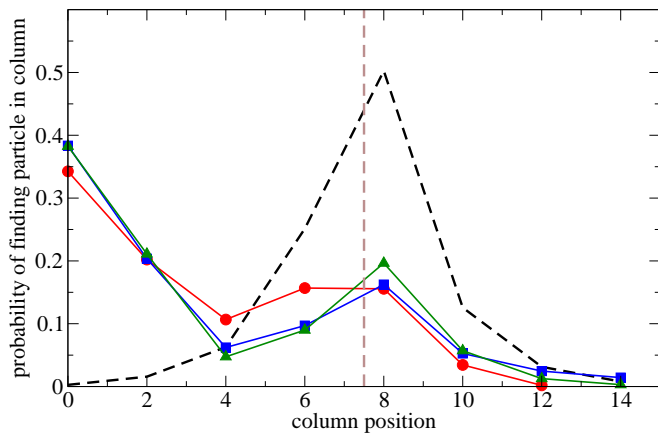


FIG. 4: As Fig. 3 but with DFT coin, after 12 (circles), 60 (squares), 120 (triangles) steps of the walk. A classical random walk after 120 steps is shown dashed.

it looks like

$$\mathbf{C}_3^{(D)} = \frac{1}{\sqrt{3}} \begin{pmatrix} 1 & 1 & 1 \\ 1 & e^{i\omega} & e^{-i\omega} \\ 1 & e^{-i\omega} & e^{i\omega} \end{pmatrix}, \quad (26)$$

where $e^{i\omega}$ and $e^{-i\omega}$ are the complex cube roots of unity. For $d=2$, the DFT coin reduces to the Hadamard coin, Eq. (13). If a DFT coin is used instead of a Grover coin on the “glued trees” graph, this keeps the amplitude near the starting point and the walk does not spread out even as far as a classical random walk, see Fig. 4. While this is not useful in the context of the “glued trees” problem, it is still highly non-classical behaviour, and with the right problem and initial coin state, the DFT coin operator may find its place in a useful quantum walk algorithm.

IV. GRAPHS OF DEGREE FOUR

Quantum walks on regular two dimensional lattices have been investigated numerically by Mackay *et al.* [26]. They found that the choice of coin operator gave different prefactors to the linear spreading rate of the quantum walk (compared to quadratic classically) and showed some different symmetries for different coin operators.

Here we present a more systematic (but by no means comprehensive) investigation of the effects of different unbiased coin operators combined with different initial states. We consider mainly an unbounded, regular, square lattice, but also consider the cases where the edges are joined in either normal periodic boundary conditions to give a torus, or twisted to give a Klein bottle.

A. Quantum Walk on a Two Dimensional Lattice

One obvious generalisation of a Hadamard coin to two spatial dimensions is to take two Hadamard coins, one

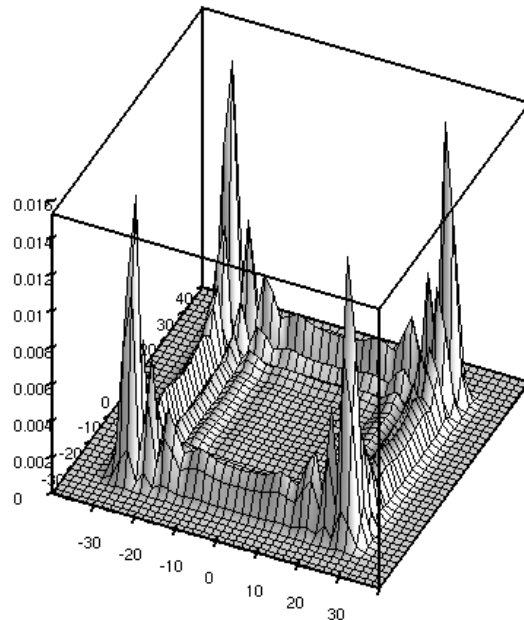


FIG. 5: Distribution obtained after 40 steps of a quantum walk on a square lattice using a Hadamard coin operator and the symmetric initial state Eq. (29).

for left or right ($|L\rangle$, $|R\rangle$), and one for up or down ($|U\rangle$, $|D\rangle$). As shown in [26], this simply produces the same pattern as the Hadamard coined walk on a line in both directions, because the coin operator does not mix the two directions in any way, see Fig. 5. The standard deviation is the same for all choices of initial state that produce a symmetric distribution, even maximally mixed, and is $\sqrt{2}$ larger than the standard deviation for the walk on the line, as noted by Mackay *et al.* [26].

More interesting are the degree-4 DFT coin,

$$\mathbf{C}_4^{(D)} = \frac{1}{2} \begin{pmatrix} 1 & 1 & 1 & 1 \\ 1 & i & -1 & -i \\ 1 & -1 & 1 & -1 \\ 1 & -i & -1 & i \end{pmatrix}, \quad (27)$$

and degree-4 Grover coin,

$$\mathbf{C}_4^{(G)} = \frac{1}{2} \begin{pmatrix} -1 & 1 & 1 & 1 \\ 1 & -1 & 1 & 1 \\ 1 & 1 & -1 & 1 \\ 1 & 1 & 1 & -1 \end{pmatrix}, \quad (28)$$

(the only case where the Grover coin is unbiased), both used in Ref. [26]. Typical results for these coins and a symmetric initial coin state

$$\begin{aligned} |\psi_0^{(\text{sym})}\rangle &= \frac{1}{2} (|LD\rangle + i|LU\rangle + i|RD\rangle - |RU\rangle) \otimes |0\rangle \\ &= \frac{1}{2} (|L\rangle + i|R\rangle) \otimes (|D\rangle + i|U\rangle) \otimes |0\rangle, \end{aligned} \quad (29)$$

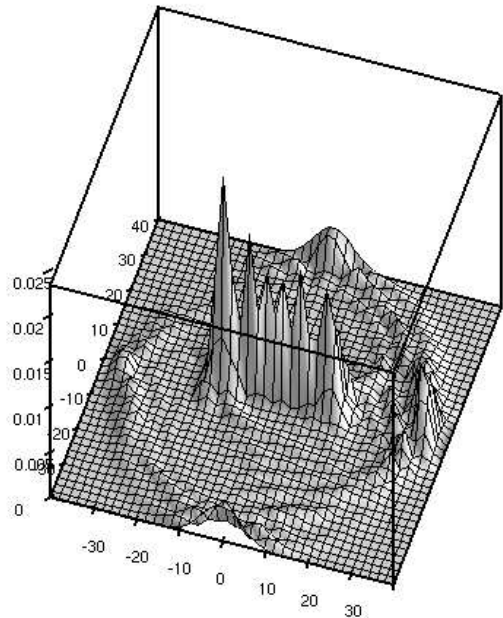


FIG. 6: Distribution obtained after 40 steps of a quantum walk on a square lattice using a DFT coin operator and the symmetric initial state Eq. (29).

with the particle starting at the origin are shown in Figs. 6 and 7.

As noted in Sec. II, there is essentially only one type of coin operator for the quantum walk on a line, the Hadamard operator, with the full range of outcomes accessible by adjusting the coin initial state. For the walk on a two dimensional lattice, the situation is obviously more complicated: the three coins illustrated so far give distinctly different results whatever initial coin state is chosen. The full range of possibilities is determined by the $SU(4)$ group structure of the unitary coin operator, but in order to sample the possibilities numerically, we chose to look at unbiased coins (all elements have modulus one half) and to further restrict those elements to be $\pm 1/2$ or $\pm i/2$. Choosing the leading diagonal entry to be $+1/2$ leads to a set of 640 such unitary coin operators, however, there is a high degree of redundancy if one groups all results that are the same apart from rotation or reflection. This can be done by using a simple initial state of (say) $|RU\rangle$, and recording the second moment of the distribution. The 640 coin operators then fall into just 10 types, with either 32, 64 or 128 coin operators of the original 640 in each type (more symmetric distributions have fewer variations). The Hadamard, Grover and DFT coin operators are all of different types.

We then varied the initial state of the coin, and looked for the maximum and minimum second moments. These always occurred for symmetric distributions (zero first moment), the second moment is thus equal to the variance in these cases. Our results contradict those of

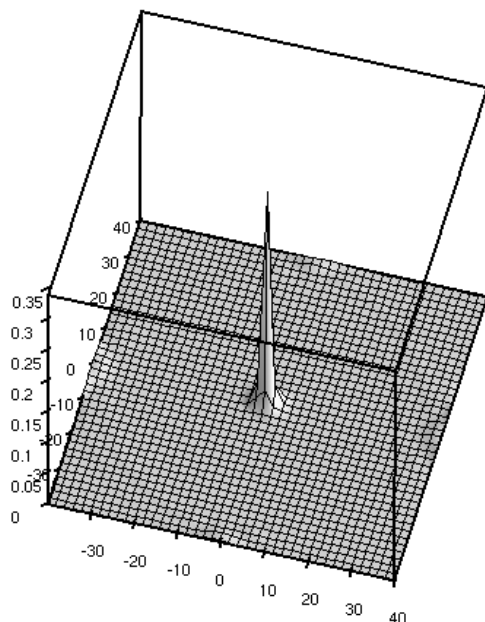


FIG. 7: Distribution obtained after 40 steps of a quantum walk on a square lattice using a Grover coin operator and the symmetric initial state Eq. (29).

Mackay *et al.*, whose choices of initial states did not fully exploit the properties of the Grover coin. Out of the ten types, the Grover type coin can produce both the maximum and minimum possible second moments, meaning that depending on the initial state, it can either spread fastest or slowest from the starting point. The distributions make clear why, see Fig. 7. They have an imperfect circular symmetry on the square lattice, with a central spike, and a ring with something like the profile of the distribution of the walk on a line superimposed on it. The different initial states control how much of the distribution is in the central spike and how much is in the ring, leading to the minimum and maximum values of the standard deviation. In fact, most of the distribution ends up in the central spike, except for exactly the right choice of initial state,

$$|\psi_0^{(G)}\rangle = \frac{1}{2} (|LD\rangle - |LU\rangle - |RD\rangle + |RU\rangle). \quad (30)$$

Figure 8 shows the distribution produced from this initial state, the contrast with Fig. 7 due to the absence of the central spike is striking (though note the vertical axes have different scales). Shenvi *et al.* exploit this property of the Grover operator in a different way in their quantum walk search algorithm [9]. Here they perturb the coin operator by applying a different operation just at one marked vertex. This causes an initially uniform particle distribution over the whole lattice to converge on the marked vertex, the reverse of a quantum walk starting at the origin and spreading out.

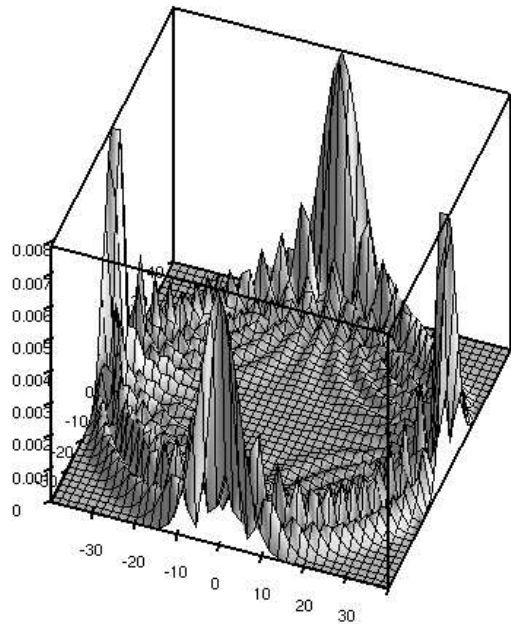


FIG. 8: Distribution obtained after 40 steps of a quantum walk on a square lattice using a Grover coin operator and the symmetric initial state Eq. (30).

A DFT coin is not so symmetric (at most rotationally symmetric through π , whereas both Hadamard and Grover coin operators can produce distributions rotationally symmetric through $\pi/2$), but with the right choice of initial condition, it too can produce a ring shape with no central spikes, see Fig. 9. The initial state that produces this distribution is

$$|\psi_0^{(D)}\rangle = \frac{1}{2} \left(|LD\rangle + \frac{1-i}{\sqrt{2}} |LU\rangle + |RD\rangle - \frac{1-i}{\sqrt{2}} |RU\rangle \right). \quad (31)$$

The results presented by Mackay *et al.* [26] did not test a sufficiently wide range of initial states to draw representative conclusions about the effects of entangled coins on the distributions obtained for the quantum walks. They attributed faster spreading to lack of entanglement between the coin directions. However, the differences we have found between Hadamard coins and Grover or DFT coins are not in the degree of spread per se, but in the extent to which this can be varied simply through varying the initial coin state. Both the Grover and DFT coins produce faster spreading than the Hadamard coins with the initial states noted above.

B. Cycles in two dimensions

By joining a square or rectangular section of a two dimensional lattice at opposite edges, the walk space becomes periodic in both directions. In one dimension there

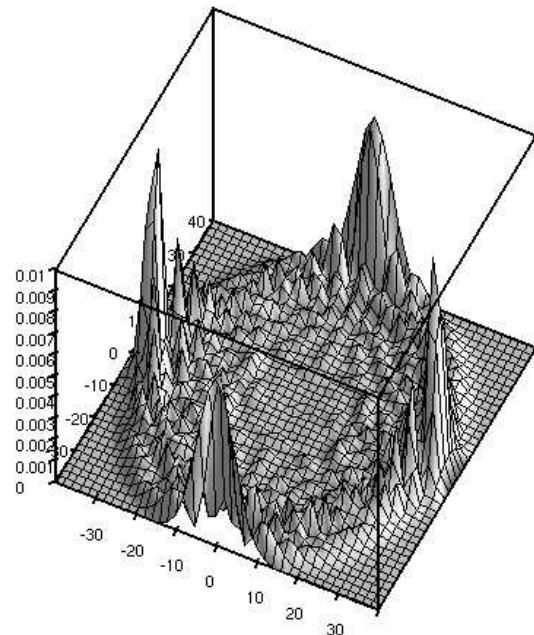


FIG. 9: Distribution obtained after 40 steps of a quantum walk on a square lattice using a DFT coin operator and the symmetric initial state Eq. (31).

is only the N -cycle, but in two dimensions the edges can be joined directly, or twisted like a Möbius strip. This gives three structures that are two dimensional analogues of the N -cycle, a torus, a closed Möbius strip, and a Klein bottle, depending on whether none, one, or both pairs of the edges are joined twisted. Periodic boundary conditions of these types are easy to implement numerically. We tested a range of such structures using the same coins as for the walk on a lattice, and found similar results to those for a walk on a N -cycle with respect to mixing times and limiting distributions. Further results for two dimensional cycles are presented at the end of Sec. VI.

V. GRAPHS OF HIGHER DEGREE

For completeness, we mention that the hypercube, first studied by Moore and Russell [20], and later found by Kempe [21] to illustrate the possibility of an exponential speed up with quantum walks, uses a higher dimensional coin. A hypercube with 2^N vertices has exactly N connections to each vertex and thus requires a N dimensional coin Hilbert space. Shenvi *et al.* [9] also based their quantum walk search algorithm on a hypercube, though as they note, other lattices, such as a square lattice, will do equally well. The symmetry of the hypercube with a Grover coin is such that with a symmetric initial state, the whole problem may be mapped to a walk on a line with a variable coin operator, in the same way as for the “glued trees” graph (see Sec. III). Consequently, there is

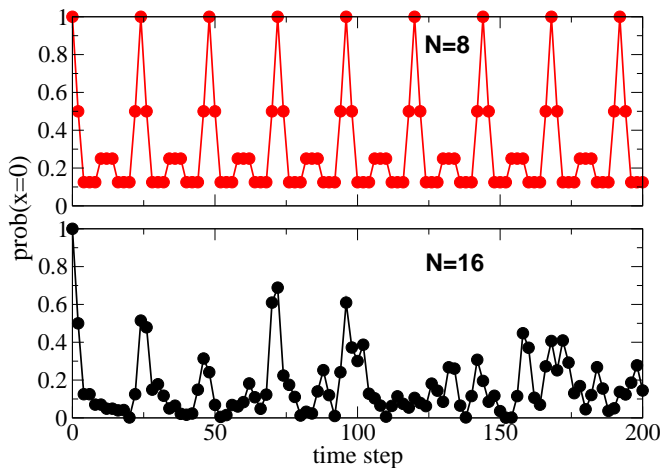


FIG. 10: Probability of finding the particle at its initial position ($x=0$) for cycles of size $N = 8$ (upper) and $N = 16$ (lower) plotted against the time step of the quantum walk using a Hadamard coin. Only even time steps are plotted, since for odd time steps the probability of finding the particle at an even numbered node is zero.

a wide range of possibilities with less symmetric higher dimensional coins yet to be explored.

VI. PERIODICITY IN QUANTUM WALKS

Systematic study of a quantum walk on a N -cycle, (described in Sec. II B), shows that among the smaller values of N , a number of completely periodic walks arise. This is the opposite property to mixing: here the walk returns exactly to its initial state after a finite number of steps Ω , whereupon it repeats the same set of steps and returns exactly again after 2Ω steps, and so on. There is no classical analogue of this property for random walks, since in the classical case the dynamics are not deterministic. A classical random walk on a cycle will return to its starting state at irregular, unpredictable times. Note too, that this periodicity is not connected with whether the limiting distribution is uniform or not, since here we are concerned with exact return to the initial state, rather than the time-averaged quantity in Eq. (18). Related ideas in continuous time walks have been studied by Ahmadi *et al.* [28], where they are concerned with exact instantaneous uniform mixing, rather than exact instantaneous return to the initial state.

Using a Hadamard coin, the “cycle” of size $N = 2$ is trivially periodic, returning to its original state after two steps. A cycle of size $N = 4$ has a period of eight steps. This was first noted by Travaglione and Milburn [29]. The cycle with $N = 8$ has a period of 24 steps, but $N = 16$ is chaotic and does not return to its initial state exactly even after many thousands of steps. This is illustrated in Fig. 10, where the probability of the particle being at its initial position is plotted as a function of the

TABLE I: Known periods in a walk on a cycle. Coin phase $\delta = 0$ unless specified.

N	period Ω	bias in coin ρ
2	2	$\frac{1}{2}$
3	12	$\frac{1}{3}, \delta = \frac{\pi}{3}$
4	8	$\frac{1}{2}$
5	60	$\left(\frac{\sin(\pi/6)}{\sin(\pi/5)}\right)^2, \delta = \frac{3\pi}{5}$
6	12	$\frac{1}{3}$
8	24	$\frac{1}{2}$
10	60	$\left(\frac{\sin(\pi/6)}{\sin(\pi/5)}\right)^2 \simeq 0.7236$
16	chaotic	$\frac{1}{2}$

time step. A probability of one is an exact return to the initial state (modulo the coin state, which is not shown here, but does also, in fact, return to exactly the initial state). If the coin is allowed to be biased, then a few more periodic examples can be found, $N = 6$ with period 12, and $N = 10$ with period 60. With judicious choice of phases in place of the Hadamard phases of $\theta = \phi = 0$, $N = 3$ has a period of 12, and $N = 5$ has a period of 60, clearly related to $N = 6$ and $N = 10$ respectively, but these were the only odd- N cycles we found. These results are summarised in Table I.

The condition that must be satisfied for exact periodicity is obtained from Eq. (11), which also holds for the walk on a cycle if the appropriate forms for the eigenvalues and eigenvectors are substituted. The wavefunctions $|\psi_t\rangle$ at two different times, t and $t + \Omega$ are set equal, giving

$$(\lambda_k^\pm)^\Omega = 1 \quad \forall k \in \{0, 1 \dots N-1\}. \quad (32)$$

Using Eq. (16) gives

$$\begin{aligned} (\delta + \omega_k)\Omega &= 2\pi j_+, \\ (\delta - \omega_k + \pi)\Omega &= 2\pi j_-, \end{aligned} \quad (33)$$

where j_\pm are integers. Substituting these into Eq. (17) gives

$$\cos\left(\frac{\pi j}{\Omega}\right) = \sqrt{\rho} \cos\left(\frac{2\pi k}{N} - \frac{\pi m}{\Omega}\right) \quad \forall k, \quad (34)$$

where ρ is the bias in the coin operator, m is an integer specifying the relative phases in the coin operator through $m\pi/\Omega - \pi/2 = \delta = (\theta + \phi)/2$, k is the integer Fourier variable, and j is an integer that can be different for each k , but must be odd or even to match whether m is odd or even. Clearly, the larger N is, the harder it is to find solutions for Eq. (34) for all k at the same time (apart from the trivial solutions for $\rho = 0$ or 1). We do not know if we have found all possible solutions that give periodic quantum walks on a cycle, but we conjecture that there are only a finite number of such solutions and that we have found nearly all if not all of them.

We also studied periodicity on two dimensional cycles, as described in Sec. IV B. With a Hadamard coin and a torus made from suitable small dimensions, periodicity is also obtained in the cases predictable from Table I. For a closed Möbius strip or Klein bottle, the twisted dimension is only periodic if the size is half that in Table I, because the twist causes the walk to traverse the cycle twice before returning to its initial state. The Grover coin shows the same periodicities as the Hadamard coin. However, a DFT coin only shows periodicity for a torus of dimensions 4×4 , and not at all on the twisted surfaces. This is due to the asymmetry of the DFT coin compared to the Grover and Hadamard coins. During the double circuit of the twisted surface, the wavefunction interferes with a mirror image of itself, so periodicity will only be observed with coins that produce suitably mirror symmetric distributions.

VII. SUMMARY

We have studied discrete, coined quantum walks on regular lattices, in one and two spatial dimensions (graphs with vertices of degree two, three and four). Both the bias (away from equal probability of choosing each direction) and the phases in the coin operator, and the initial state of the coin, can be used to control the evolution of the quantum walk. In a quantum walk on a line, we have found a biased initial state of the coin which produces a higher degree of asymmetry than the simple $|L\rangle$ or $|R\rangle$ initial states. The same bias produces a symmetric distribution when combined with the opposite phase between the coin components. This illustrates two distinct ways to obtain the same symmetric distribution, by interference, and by combination of two orthogonal biased distributions each a mirror image of the other. In a quantum walk on a cycle, we have determined the condition

for mixing to a uniform limiting distribution, for a general coin operator and initial state. Non-uniform limiting distributions are highly sensitive to decoherence, so to make use of the properties of such walks, it will be best to measure effects that occur after a reasonably short number of steps of the walk. Quantum walks of degree three have a more interesting choice of coin operators, an example in which a Grover coin solves a problem (“glued trees”) efficiently, while a DFT coin stays nearer the starting point than even a classical random walk illustrate the range of possibilities to be explored. Numerical study of regular lattices in two dimensions (degree-4 graphs) show that the Grover and DFT coins have interesting properties independent of the symmetry of the lattice (circular spreading on a square lattice). Suitable choice of initial state makes the Grover coin spread fastest or slowest out of all the coin operators tested, in contrast to the conclusions in [26], where only a few initial states were tested. Finally, a small set of exactly periodic quantum walks on cycles of sizes 2, 3, 4, 5, 6, 8, and 10 have been found, and the condition on which this exact periodicity depends derived. Such periodicities are of interest in their own right, and we also suggest that it may be possible to exploit them to pick out small scale regularities in larger structures.

Acknowledgments

We thank Julia Kempe, Peter Knight, and Jiannis Pachos for useful discussions. VK thanks the Mathematical Science Research Institute in Berkeley, CA, for hospitality during the Quantum Computing Program in Fall 2002, and the participants of that programme for many stimulating discussions. BT and VK funded by the UK Engineering and Physical Sciences Research Council.

-
- [1] E. Farhi and S. Gutmann, Phys. Rev. A **58**, 915 (1998), quant-ph/9706062.
 - [2] Y. Aharonov, L. Davidovich, and N. Zagury, Phys. Rev. A **48**, 1687 (1992).
 - [3] D. A. Meyer, Phys. Lett. A pp. 337–340 (1996), quant-ph/96004011.
 - [4] D. A. Meyer (1996), quant-ph/9605023.
 - [5] D. A. Meyer, J. Stat. Phys. **85**, 551 (1996), quant-ph/9604003.
 - [6] D. Aharonov, A. Ambainis, J. Kempe, and U. Vazirani, in *Proc. 33rd STOC* (Assoc. for Comp. Machinery, New York, 2001), pp. 50–59, quant-ph/0012090.
 - [7] A. Ambainis, E. Bach, A. Nayak, A. Vishwanath, and J. Watrous, in *Proc. 33rd STOC* (Assoc. for Comp. Machinery, New York, 2001), pp. 60–69.
 - [8] A. M. Childs, R. Cleve, E. Deotto, E. Farhi, S. Gutmann, and D. A. Spielman (2002), quant-ph/0209131.
 - [9] N. Shenvi, J. Kempe, and K. B. Whaley, Phys. Rev. A **67**, 052307 (2003), quant-ph/0210064.
 - [10] M. Jerrum, A. Sinclair, and E. Vigoda, in *Proc. 33rd STOC* (Assoc. for Comp. Machinery, New York, 2001), pp. 712–721.
 - [11] U. Schöning, in *40th Annual Symposium on Found. of Comp. Sci.* (IEEE Computer Society Press, Los Alamitos, CA, 1999), pp. 17–19.
 - [12] M. Dyer, A. Frieze, and R. Kannan, J. of the ACM **38**, 1 (1991).
 - [13] R. Motwani and P. Raghavan, *Randomized Algorithms* (Cambridge University Press, Cambridge, UK, 1995).
 - [14] E. Bach, S. Coppersmith, M. P. Goldschen, R. Joynt, and J. Watrous (2002), quant-ph/0207008.
 - [15] H. A. Carteret, M. A. Ismail, and B. Richmond (2003), quant-ph/0303105.
 - [16] T. Yamasaki, H. Kobayashi, and H. Imai, in *Unconventional Models of Computation, Third International Conference, UMC 2002, Kobe, Japan, October 15-19, 2002, Proceedings*, edited by C. Calude, M. J. Dinneen, and F. Peper (Springer, 2002), vol. 2509 of *Lecture Notes*

- in Computer Science*, pp. 315–330, ISBN 3-540-44311-8, quant-ph/0205045.
- [17] V. Kendon and B. Tregenna, *Phys. Rev. A* **67**, 042315 (2003), quant-ph/0209005.
- [18] T. A. Brun, H. A. Carteret, and A. Ambainis, *Phys. Rev. A* **67**, 052317 (2003), quant-ph/0210161.
- [19] T. A. Brun, H. A. Carteret, and A. Ambainis, *Phys. Rev. A* **67**, 032304 (2003), quant-ph/0210180.
- [20] C. Moore and A. Russell, in *Proc. 6th Intl. Workshop on Randomization and Approximation Techniques in Computer Science (RANDOM '02)*, edited by J. Rolim and S. Vadhan (Springer, 2002), pp. 164–178, quant-ph/0104137.
- [21] J. Kempe (2002), quant-ph/0205083.
- [22] J. Kempe, *Contemp. Phys.* **44** (2003), to appear, quant-ph/0303081.
- [23] N. Konno, *Quantum Information Processing* **1**, 345 (2002), quant-ph/0206053.
- [24] N. Konno (2003), private communication.
- [25] M. Bednarska, A. Grudka, P. Kurzyński, T. Luczak, and A. Wójcik (2003), quant-ph/0304113.
- [26] T. D. Mackay, S. D. Bartlett, L. T. Stephenson, and B. C. Sanders, *J. Phys. A: Math. Gen.* **35**, 2745 (2002), quant-ph/0108004.
- [27] J. Watrous (2002), private communication.
- [28] A. Ahmadi, R. Belk, C. Tamon, and C. Wendler (2002), quant-ph/0209106.
- [29] B. C. Travaglione and G. J. Milburn, *Phys. Rev. A* **65**, 032310 (2002), quant-ph/0109076.